

Laser oscillation with optically pumped very thin GaAsAl_xGa_{1-x}As multilayer structures and conventional double heterostructures

R. C. Miller, R. Dingle, A. C. Gossard, R. A. Logan, W. A. Nordland et al.

Citation: *J. Appl. Phys.* **47**, 4509 (1976); doi: 10.1063/1.322422

View online: <http://dx.doi.org/10.1063/1.322422>

View Table of Contents: <http://jap.aip.org/resource/1/JAPIAU/v47/i10>

Published by the [American Institute of Physics](#).

Related Articles

Note: A large aperture four-mirror reflective wave-plate for high-intensity short-pulse laser experiments
Rev. Sci. Instrum. **83**, 036104 (2012)

Time-resolved single-shot imaging of femtosecond laser induced filaments using supercontinuum and optical polarigraphy
Appl. Phys. Lett. **100**, 111107 (2012)

Multicolor Čerenkov conical beams generation by cascaded- $\chi(2)$ processes in radially poled nonlinear photonic crystals
Appl. Phys. Lett. **100**, 101101 (2012)

Influence of laser irradiated spot size on energetic electron injection and proton acceleration in foil targets
Appl. Phys. Lett. **100**, 074105 (2012)

MeV negative ion source from ultra-intense laser-matter interaction
Rev. Sci. Instrum. **83**, 02A710 (2012)

Additional information on J. Appl. Phys.

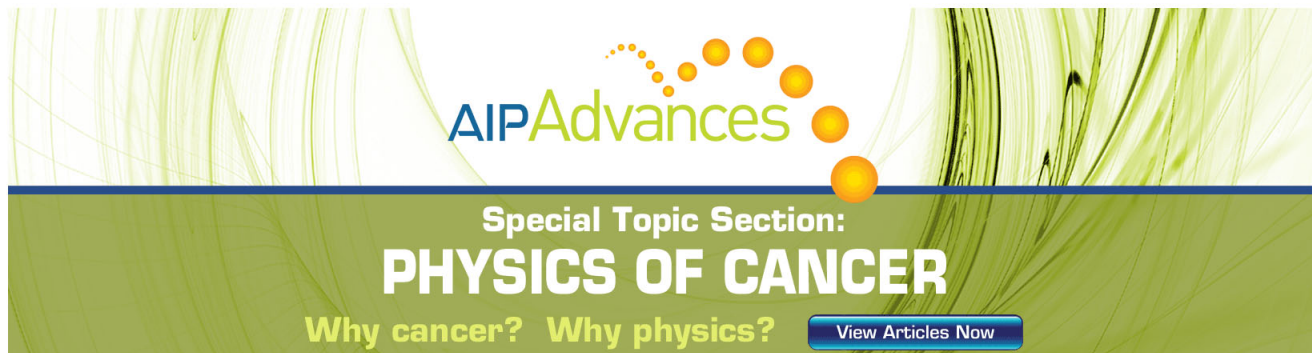
Journal Homepage: <http://jap.aip.org/>

Journal Information: http://jap.aip.org/about/about_the_journal

Top downloads: http://jap.aip.org/features/most_downloaded

Information for Authors: <http://jap.aip.org/authors>

ADVERTISEMENT



AIP Advances

Special Topic Section:
PHYSICS OF CANCER

Why cancer? Why physics? [View Articles Now](#)

Laser oscillation with optically pumped very thin GaAs-Al_xGa_{1-x}As multilayer structures and conventional double heterostructures

R. C. Miller, R. Dingle, A. C. Gossard, R. A. Logan, W. A. Nordland, Jr., and W. Wiegmann

Bell Laboratories, Murray Hill, New Jersey 07974
(Received 16 April 1976; in final form 18 June 1976)

Optically pumped laser oscillation from multilayer heterostructures (ML) grown by molecular beam epitaxy (MBE) that consist of many alternating thin layers of GaAs and Al_xGa_{1-x}As has been studied in some detail over the temperature range 7–300 K. These samples which have GaAs layers 100–200 Å thick that act as one-dimensional potential wells for electrons and holes have thresholds for lasing that are generally a factor of 2 or more higher than conventional comparable GaAs-Al_xGa_{1-x}As double heterostructures (DH) also grown by MBE. The quantum effects due to the GaAs wells of the ML samples are shown to exist under lasing conditions well above room temperature, but there is no evidence to date of the beneficial effects expected from the modified density of states of this type of structure. Also optically pumped conventional DH lasers grown by MBE and liquid phase epitaxy (LPE) have been compared. The DH lasers grown by MBE are found to have lasing thresholds that are consistently about a factor of 2 higher than their twins grown by LPE.

PACS numbers: 42.60.Jf, 42.50.+q, 78.65.+t

INTRODUCTION

A recent paper¹ disclosed laser action from optically pumped heterostructures consisting of many alternating layers of GaAs and Al_{0.2}Ga_{0.8}As. The active GaAs layers which were very thin, 80 Å, and separated by Al_{0.2}Ga_{0.8}As layers, 240 Å thick, served as one-dimensional potential wells for electrons and holes with a discrete number of bound energy levels within the wells.² Previous studies of the absorption spectrum of these structures have shown that the depths of the potential wells for electrons and holes are 0.22 and 0.03 eV, respectively.² Recombination between electrons and holes that occupy the lowest bound states in the wells gives rise to radiation at energies above the bulk GaAs-energy gap. The Al_{0.2}Ga_{0.8}As layers were sufficiently thick in the samples studied so that tunneling^{3,4} between the thin GaAs layers should not occur. However, the emitted radiation penetrates deeply into the intervening Al_{0.2}Ga_{0.8}As regions. Thus in this type structure, the electrons are highly confined to the GaAs layers while the optical fields are shared by all the layers. Since the multilayers just described were sandwiched between 2-μm-thick layers of Al_{0.2}Ga_{0.8}As, the multilayer region acted as a waveguide for the generated light. Such structures have exhibited laser action under intense optical excitation from a tunable optical parametric oscillator but only at very low temperatures.¹ A multilayer structure and the configuration used to obtain laser oscillation are indicated schematically in Fig. 1. Observed thresholds reported were equivalent to approximately 36 kA/cm² at 15 K. These initial results were disappointing in that the observed laser thresholds were very high and gave no indication of the beneficial effects that one might expect from the modified density of states of these structures.² However, in agreement with expectations,¹ these structures did lase at a wavelength (8070 Å) determined by the depth of the GaAs wells.

This paper describes additional data on the active characteristics of these and similar multilayer struc-

tures (ML), and some comparisons are made with optically pumped conventional GaAs-Al_xGa_{1-x}As double-heterostructures (DH) lasers grown both by molecular beam epitaxy (MBE) and liquid phase epitaxy (LPE). The new data on the ML include the temperature dependence of the lasing threshold and generated wavelengths, observations of the longitudinal mode structure, absolute and differential quantum efficiencies, threshold measurements on samples of different lengths to indicate optical losses and gain characteristics, and absorption under conditions of low and high excitation, plus spontaneous photoluminescence spectra, near the band gap at very low temperatures.

EXPERIMENTAL

The multilayer samples were undoped and grown by the MBE technique as described in detail previously.^{2,5}

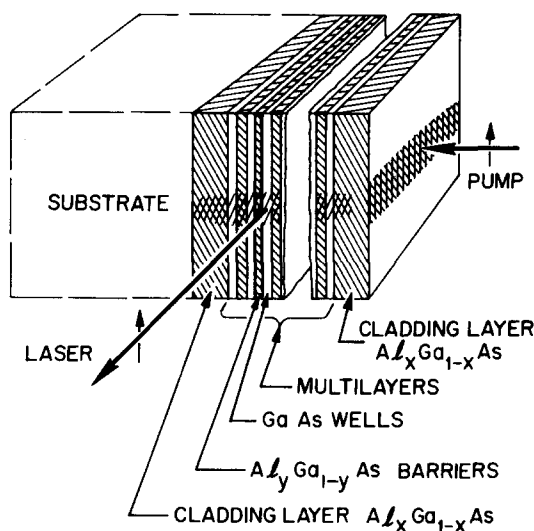


FIG. 1. Schematic drawing showing laser emission from an optically pumped multilayer structure. For the structures investigated in this study, $x=y$.

TABLE I. Structure characteristics for the multilayer and double-heterostructure samples investigated.

Sample	Multilayers		Al _x Ga _{1-x} As Barriers		Cladding		Sample length (cm)
	GaAs wells Width (Å)	Number	Width (Å)	x	Width (μm)	x	
9-5-75	188	25	19	0.3	3.0	0.3	0.101
10-1-75	116	50	64	0.22	2.5	0.22	0.105
4-10-74-SS ^a	92	40	345	0.2	3.1	0.2	0.039
4-10-74-I ^a		40	345	0.2	3.1	0.2	0.078
4-10-74-L ^a		40	345	0.2	3.1	0.2	0.173
4-15-75 ^a	191	26	175	0.20	2.0	0.20	0.1
Double heterostructures							
	Growth method		GaAs width (μm)				
7-17-75	MBE		0.53		2.6	0.3	0.1
LP-1141	LPE		0.50		2.1	0.33	0.1

^aAnnealed in As atmosphere 2 h at 850 °C.

Bulk GaAs (layers $\geq 1000 \text{ \AA}$) grown under the same conditions is p type $\approx 10^{14}/\text{cm}^3$. Relevant parameters for the various samples investigated are given in Table I. Note that the Al_xGa_{1-x}As barriers are thin enough in 9-5-75 and 10-1-75 to produce superlattice-type structures.^{3,4} All the samples except those designated with 4-10-74 were grown with a new system which has an improved cryopanel to prevent outgassing of the ovens and the surrounding room temperature walls onto the sample. In addition, the new system has superior ion pumps. In all cases, the laser mirrors consisted of cleaved {110} faces. For most of the observations, the samples were mounted with a thin layer of rubber cement onto a copper block affixed to the tip of a variable-temperature Cryotip He refrigerator.

The tunable output of a Chromatix optical parametric oscillator, usually pumped by the second harmonic of the 1.0642-μm Nd:YAG line, was focused by means of either one or two cylindrical lenses onto the broad-area face of the sample to be excited as indicated schematically in Fig. 2. The pumped face was parallel to the layer planes as depicted in Fig. 1. The 30-cm focal length lens was adjusted so that the width of the focused spot coincided with the sample length, while the 10-cm focal length lens was positioned to give the largest output signal and hence the lowest threshold. This pumping scheme has been exploited earlier by Chinn *et al.*⁶ and Rossi *et al.*⁷ in their work on optically pumped GaAs and GaAs-Al_xGa_{1-x}As DH lasers. The tunable oscillator had a maximum output of about 400 W which was attenuated to the desired power level by adjusting the middle of three Glan polarizers placed in series as indicated in Fig. 2. The parametric oscillator pump pulses were 100 ns in duration for most of the experiments and occurred at a rate of 50 pps. Their spectral width was less than 1 cm^{-1} .

The output from the GaAs-Al_xGa_{1-x}As lasing structure could be collected with a lens and observed directly by means of an infrared image convertor, or directed into either a large-area Si photocell or a 1/2-m Jarrell-Ash spectrometer.

RESULTS

This section is divided into five parts which encompass the major areas of data acquisition, namely, lasing threshold determinations, lasing wavelengths as a function of temperature, the longitudinal mode structure, some effects of high optical pumping intensities, and absolute conversion efficiencies along with their ramifications.

Threshold measurements

Lasing thresholds for both DH and ML samples were determined as a function of temperature. For both types of samples, the threshold increases by a little more than one order of magnitude as the temperature increases from 7 to 300 K. The thresholds are highest for the ML samples and increase with decreasing GaAs well thickness. In addition, the thresholds for the MBE DH units are about twice those of their LPE twins.

Thresholds for laser action were determined in several ways. Figure 3 shows a plot of the relative output from ML sample 4-10-74-I versus the total pump energy at 7235 Å absorbed by the thin 92-Å GaAs layers.

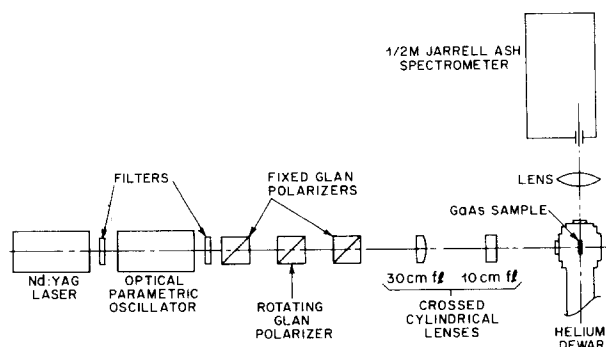


FIG. 2. Schematic drawing illustrating the experimental arrangement for optically pumping the ML and DH lasers. The three Glan polarizers serve as a variable attenuator of the optical pump. Focusing conditions were sometimes varied from that shown in the figure.

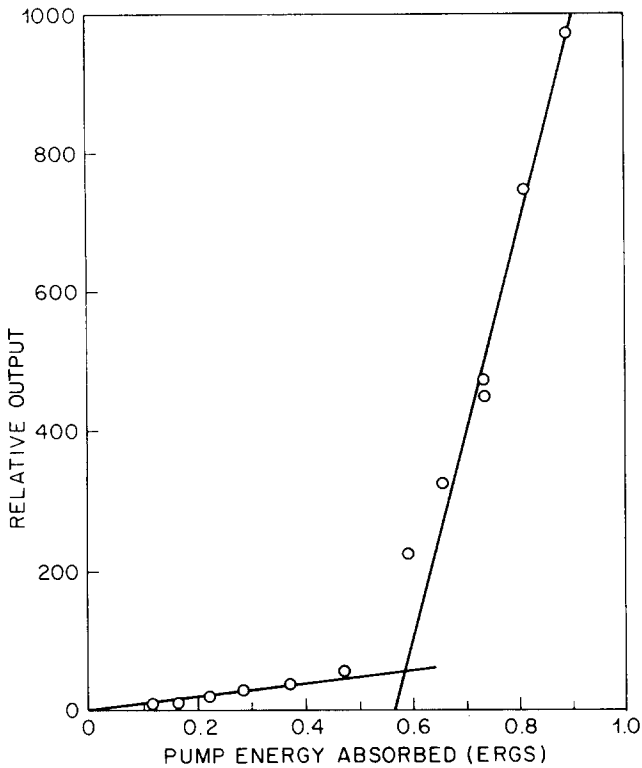


FIG. 3. Relative output versus pump energy absorbed by the thin GaAs layers at 6 K for ML 4-10-74-I.

These data, obtained at 6 K with a detected spectral width of about 5 Å centered on the emission peak, give a threshold of 0.57 erg which is equivalent to 5.4 kA/cm² when the measured focal area (6.5×10^{-5} cm²) and pulse duration (0.1 μs) are taken into account. The threshold can also be detected visually by observing the onset of severe spiking in the output which occurs when the fluctuating pump power is very near threshold. Third, line narrowing can be observed. However, due to the fluctuating optical pump, these data are not as clean as similar data obtained using, for example, injection pumping. All three methods give the same nominal threshold. The direct visual observation technique is most useful for measurements that require many threshold determinations such as the temperature dependence of the threshold.

The thresholds measured as a function of temperature and shown in Fig. 4 were obtained visually. The pump wavelength was fixed at 7628 Å which is sufficiently long so that significant absorption in the Al_xGa_{1-x}As layers does not occur even at the highest temperatures. Data are shown for LPE and MBE DH twins, and for ML samples with 116- and 188 Å GaAs wells. The sample characteristics are given in more detail in Table I. Although some variation in these plots is observed from run to run, the general characteristics are preserved. The reproducibility of the experimental points is typically better than that suggested by the scatter of the lower temperature data for LP1141. Relative thresholds are taken to be proportional to the incident optical power required for lasing. Room-temperature low-intensity absorption measurements at 7628 Å show that the total active layers of all four samples absorb very

nearly the same fraction of incident pump light, ≈ 0.4 . The thresholds are highest for the sample with 116-Å GaAs wells (10-1-75), while the sample with 188-Å wells (9-5-75) exhibits thresholds at 300 K that are about 1.5 times those for the MBE DH. However, near 100 K, the optical pump coincides with the $n=3$ transition frequency of sample 9-5-75 and is believed to result in an *apparent* reduced threshold in this temperature region due to increased pump energy absorption which was not taken into account in plotting the figure. The thresholds for the MBE DH are about twice those for the LPE DH. A considerable volume of additional data on these and other samples support the results just described.

When the optically pumped samples areas (8.4×10^{-5} cm²) are taken into account, the equivalent current thresholds j_{th} can be determined. These data at 7 and 300 K are given in Table II. If the present threshold data are approximated above ≈ 120 K by $j_{th} \propto \exp(T/T_0)$, $T_0 = 153$ and 129 K for the LPE and MBE DH units, respectively. These values are in good agreement with similar data for cw injection pumped LPE and MBE DH lasers.⁸ The corresponding values for the two ML samples 10-1-75 and 9-5-75 are 110 and 136 K, respectively.

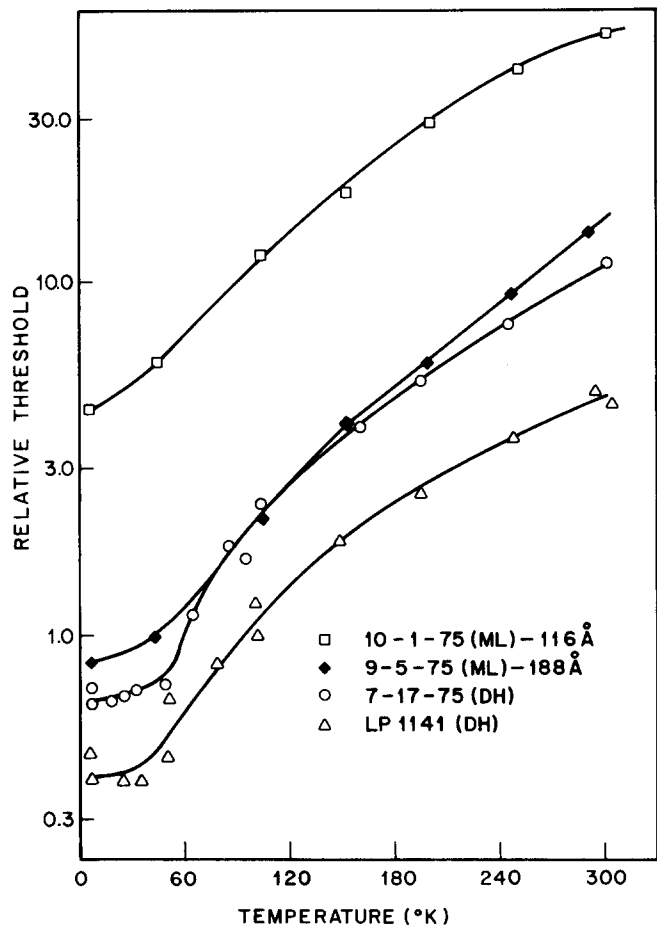


FIG. 4. Relative threshold versus temperature for two ML samples plus LPE and MBE DH twins. All samples were pumped at 7628 Å.

TABLE II. Measured thresholds j_{th} and external differential quantum efficiencies, η_e , calculated for emission from both ends of the samples.

Sample and type	Data source	6-8 K		300 K	
		j_{th} (kA/cm ²)	η_e (%)	j_{th} (kA/cm ²)	η_e (%)
4-10-74-I (ML)	Fig. 3	5.4			
LP-1141 (DH)	Fig. 4	1.9		23	
	Fig. 9			25	2.6
7-17-75 (DH)	Fig. 4	3.2		55	
	Fig. 9			83	1.2
9-5-75 (ML)	Fig. 4	4.1		75	
	Fig. 9			107	0.8
10-1-74 (ML)	Fig. 4	21		253	
	Fig. 9			323	0.3
4-10-74-SS (ML)	Fig. 11	16	13.5		
4-10-74-L (ML)	Fig. 11	2.8	14.3		

Lasing wavelengths and their temperature dependence

As discussed previously,¹ theory predicts that the lasing wavelength of the ML samples should vary with the width and depth of the GaAs wells by amounts which can be large compared to the usual wavelength variations observed¹⁰ with either doped or undoped GaAs-AlGaAs DH lasers. To test this theory, the lasing wavelengths have been determined for DH and ML samples from 7 to 450 K. As expected, it is found that the lasing wavelength decreases with decreasing GaAs well width. In addition, one of the more important conclusions to be drawn from these measurements is that the quantum effects due to the GaAs wells still exist under lasing conditions even when well above room temperature.

The data in Fig. 5 illustrate for a ML sample the relation between the absorption spectrum, the photoluminescence spectrum, and the lasing wavelength. The absorption spectra near the band edge of ML-10-1-75 at 2 and 300 K were obtained using techniques described earlier.⁹ The absorption peaks due to the $n=1$ and $n=2$ bound states of the one-dimensional potential wells are clearly resolved at 2 K. The light and heavy hole $n=1$ transitions are not resolved at 300 K. Also shown in Fig. 5 are the photoluminescence spectrum (PL) at 2 K which peaks at 8065 Å as observed through the pumped face, and the lasing wavelengths (L) at 7 and 300 K, 8090 and 8695 Å, respectively. Typical PL peaks observed through the end face are shifted to longer wavelengths by 20-30 Å. This shift is probably due to self-absorption. Thus taking this shift into account, the lasing occurs at the wavelength of the end PL peak which is on the low-energy side of the $n=1$ heavy hole transition. With the excitation technique used for these data, the photoluminescent spectrum could not be observed at 300 K.

Figure 6 shows the lasing wavelengths from 7 to 300 K for two DH samples and ML units with GaAs wells

188, 116, and 92 Å wide. In each case, the wavelength plotted is the peak of the emission at a pump power about 10% above threshold which was again determined visually. The emission bandwidth broadens somewhat as the temperature is increased so that at 300 K the difference between the curves for the two DH samples is probably not significant. These data show clearly that the lasing wavelength decreases with decreasing GaAs well width. Also shown for 10-1-75 are the temperature dependences of the spontaneous emission observed through the pumped face and the $n=1$ absorption feature taken at low excitation intensity where quantum effects are very well defined. It is evident from the data in Fig. 6 that the quantum effects due to the GaAs wells still exist under lasing conditions at 300 K. In fact, other data not shown demonstrate that these quantum effects are still present at 180°C which was the highest temperature at which lasing could be achieved with the sample studied. Furthermore, the lasing output from ML units as well as the spontaneous emission is always polarized TE, as required by radiative recombination selection rules for these structures.¹ The light generated by the DH units was not always highly polarized, in which case it presumably consisted of both TE and TM modes. Standard state-of-the-art DH injection lasers with narrow active regions, as in this work, exhibit only TE modes.^{10,11} Figure 6 also shows the GaAs band gap for undoped material calculated from the recent expression given by Thurmond.¹² These wavelength data for the DH samples are in agreement with calculations and similar results due to

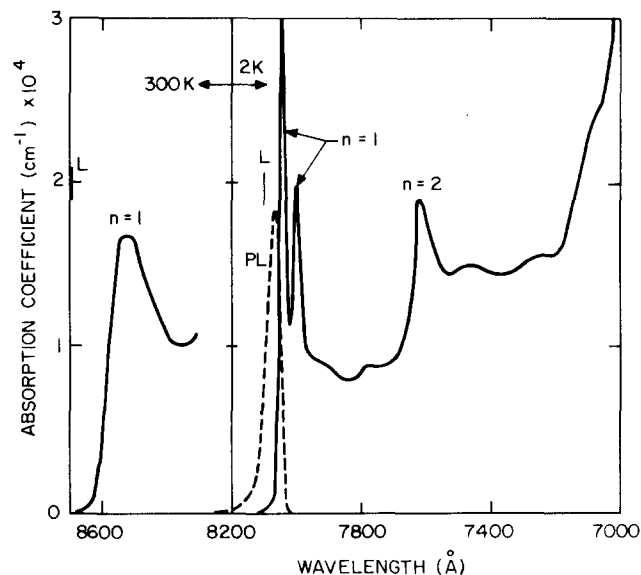


FIG. 5. Right side of figure, 2 K: Absorption spectrum of multilayer sample 10-1-75 showing exciton absorption corresponding to the $n=1$ and $n=2$ one-dimensional bound states. The absorption of the $Al_{0.22}Ga_{0.78}As$ isolation layers begins at ≈ 7100 Å. The dashed curve centered at 8065 Å is the photoluminescence (PL) spectrum observed through the pumped face, and the laser emission (L) at 7 K is shown by the vertical line at 8090 Å. Left side of figure, 300 K: Absorption spectrum of 10-1-75 showing the unresolved $n=1$ transition at the absorption edge and the laser emission wavelength (L) at 8695 Å.

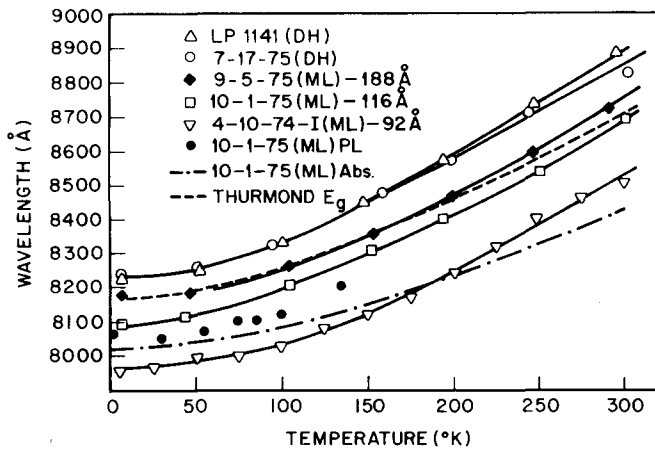


FIG. 6. Temperature dependence of the lasing energy for the four samples measured in connection with Fig. 4 and also the ML 4-10-74-I. The wavelengths of the $n=1$ absorption peak (Abs) and the photoluminescence peak (PL), both measured at low excitation levels, are also shown for 10-1-75. For comparison, the theoretical GaAs band-gap energy (E_g) determined by Thurmond is shown as a function of temperature.

others as discussed by Camassel *et al.*¹³ The energy difference $\Delta E = E_{ML} - E_{DH}$ between the lasing wavelengths for the ML 4-10-74-I and the average of the two DH samples is given as a function of temperature in Fig. 7. At the lowest temperatures, $\Delta E = 50$ meV and then it increases with T to a maximum of about 60 meV at 215 K. Since the optical pump power required increases rapidly with T , it is possible that heating of the samples shifts the emission to the long wavelength side at the higher temperatures. This effect should be most pronounced for the highest threshold samples, i. e., the multilayer structures. On the other hand, band filling effects would tend to shift the output to higher energies as the threshold increases.¹¹

Longitudinal modes

The longitudinal mode structure of ML samples has been determined and suggests that the $\text{Al}_x\text{Ga}_{1-x}\text{As}$ barriers between the GaAs wells can reduce the effects of dispersion below that characteristic of DH units.

Longitudinal modes were easily resolved with some of the ML samples at the lowest temperatures. Figure 8 shows typical data from sample 4-10-74-I. These data can be used to determine the effective group index of refraction n^* for the lasing mode from the wavelength separation $\Delta\lambda$ between modes since

$$n^* = \lambda^2 / 2l\Delta\lambda, \quad (1)$$

where λ is the lasing wavelength and l is the length of the oscillator cavity. The quantity n^* is given by

$$n^* = n - \lambda \frac{dn}{d\lambda}, \quad (2)$$

with n equal to the refractive index at wavelength λ . The average value of n^* for four different samples from the 4-10-74-I wafer is 5.0 ± 0.1 at 7 K where the average lasing wavelength is 7952 Å. In general, modes were only observable with pump powers within about a factor

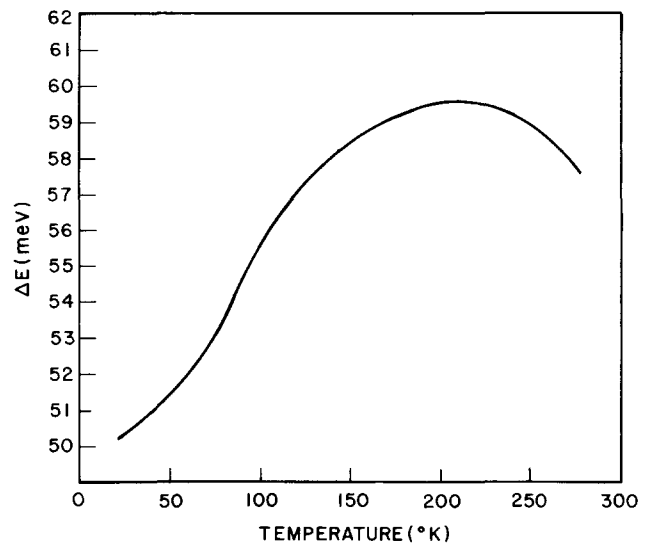


FIG. 7. Difference between the lasing energies of the ML 4-10-74-I and the average of the two DH samples versus temperature.

of 2 of the threshold power at the lowest temperatures and not observable above about 20 K. This n^* is considerably smaller than that suggested by preliminary data on $n^*(T)$ obtained during this study for optically

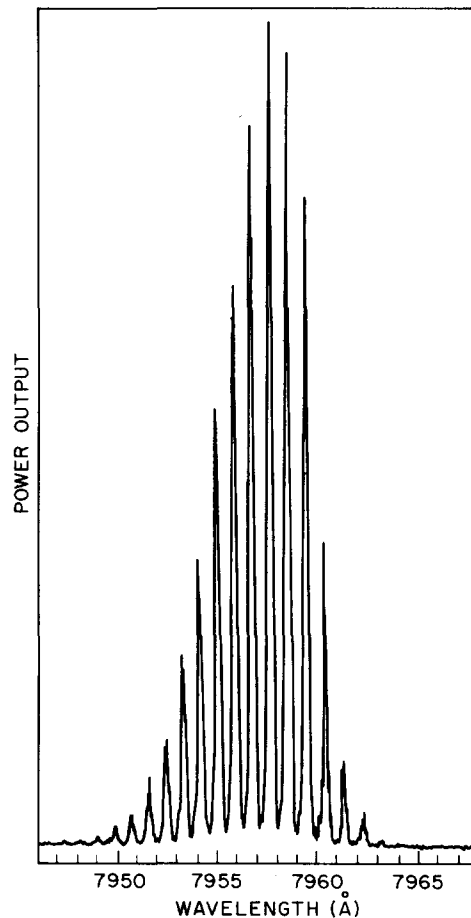


FIG. 8. Longitudinal modes observed with sample 4-10-74-I at 7 K.

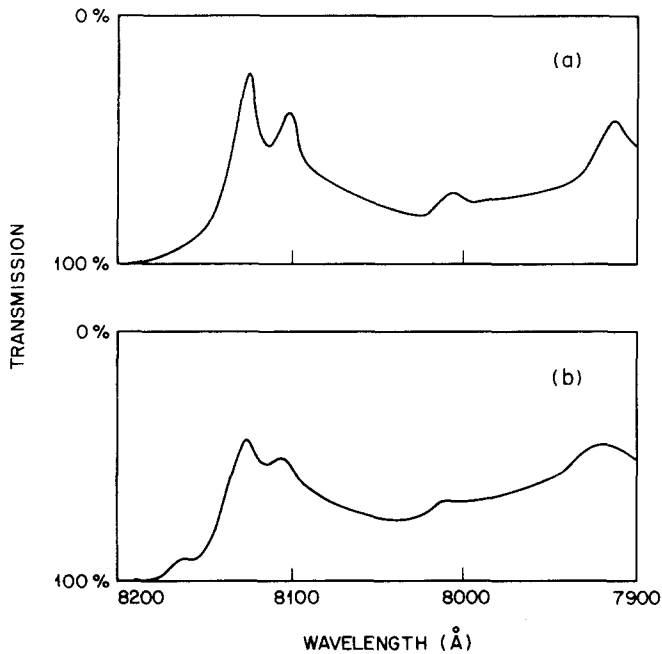


FIG. 9. Transmission versus wavelength measured at 7 K through an etched window in ML sample 4-15-75 at 1 W/cm^2 (a) and 4 kW/cm^2 (b) absorbed light intensities. The $n=1$ transitions at $\approx 8110 \text{ \AA}$, which are split due to light and heavy hole contributions, and the $n=2$ transition at $\approx 7920 \text{ \AA}$, become less pronounced at the higher intensity. The background transmission losses due to surface reflectivities and residual absorption have been subtracted out.

pumped DH lasers and an extrapolation of earlier data¹⁴ at 2 K on $n^*(\lambda)$ for injection pumped GaAs homostructure lasers. Since the waveguide for 4-10-74 consists of about 80% $\text{Al}_{0.2}\text{Ga}_{0.8}\text{As}$, it seems reasonable that its n^* should be smaller than the value for conventional structures where most of the light is in GaAs.

Effects due to high pump intensities

It is well known that some of the properties of GaAs change markedly under the high electron and hole densities, $\geq 10^{19}/\text{cm}^3$, required for stimulated emission. Under these conditions, absorption saturation and other many-body effects can occur.¹⁵ Data already discussed in connection with the temperature dependence and polarization of the emission wavelength show that the quantum states of the wells still influence the lasing characteristics at room temperature. In another experiment, the transmission of ML sample 4-15-75 that had an etched window which removed the substrate and left only the multilayers and the cladding^{2,9} was measured at both high and low incident powers to determine pump absorption of a ML sample with high electron and hole densities like those required for lasing. Data at 7 K show that at high pumping levels the $n=1$ and $n=2$ transition peaks are reduced, while the intermediate regions, where pumping is usually done, do not change significantly with pump intensity.

The measurements were made in the region of the $n=1$ ($\lambda \approx 8110 \text{ \AA}$) and $n=2$ (7920 \AA) transitions and are shown in Fig. 9. At low incident intensities [Fig. 9(a)], i. e., $\approx 1 \text{ W/cm}^2$, absorbed intensity at an energy half-

way between the heavy and light hole $n=1$ transitions, the quantum transitions are well resolved along with a weak absorption peak that has been associated with a $\Delta n=1$ forbidden transition.⁹ At high intensities [Fig. 9(b)], 4 kW/cm^2 absorbed intensity near the center of the $n=1$ transitions, all the structure due to the quantum effects associated with the GaAs wells is still present but with a reduced contrast in the region of the peaks. The additional small peak in Fig. 9(b) on the low energy side of the $n=1$ transitions is not understood. The GaAs bulk exciton and laser photon energies are both at longer wavelengths than this peak. The high incident intensity level in Fig. 9(b) is comparable to that required for laser action with this sample. These data do suggest a certain amount of saturation near the peaks. For the $n=1$ transitions the high intensity absorption coefficients for the two peaks are about 0.6 times the low intensity values.

Similar detailed data are not available for ML samples at room temperature. However, preliminary data with DH and ML units at 300 K again indicate at most a small amount of saturation in the region where the structures are typically pumped for lasing. However, this effect is small compared to other uncertainties. Since in most cases the samples were not pumped near the absorption peaks, e. g., the $n=2$ transition, intensity-dependent effects should not significantly alter the fraction of pump light absorbed by the GaAs active regions.

Absolute conversion efficiencies, absorption loss, and gain characteristics

Measurements of the light energy generated versus optical pump energy absorbed by the active GaAs layers were obtained for DH and ML samples in order to compare the differential quantum efficiencies, and to esti-

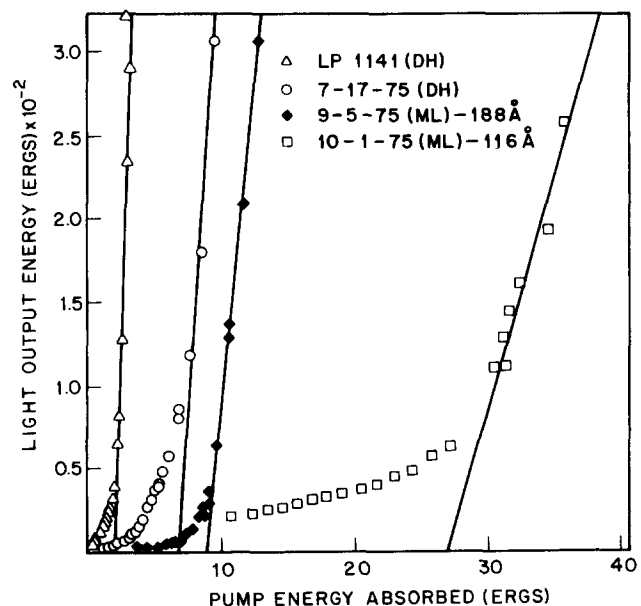


FIG. 10. Light output energy versus pump energy absorbed at 300 K for four of the samples used in connection with Figs. 4 and 6. The samples were pumped at 7628 \AA .

mate the effective loss and gain characteristics of ML units. It is found that the differential quantum efficiencies for the ML samples are inferior to those of the DH units. It appears that the effective loss of ML units can be quite low, presumably due to the highly transparent $\text{Al}_x\text{Ga}_{1-x}\text{As}$ barriers between the GaAs wells. In addition, these data for ML samples at 8 K suggest that the gain varies linearly with pump intensity as is also the case for injection pumped lasers at very low temperatures.

For these measurements, the generated light was collected with a calibrated large-area Si photocell placed as close as possible to the sample and filters required to remove scattered pump light. Appropriate factors were included in the analysis to correct for the geometry and filters. Figure 10 shows these data at 300 K for the same four samples used in connection with Figs. 4 and 6. While the time duration of the nearly triangular pump pulses at 7628 \AA is fixed, $\approx 0.1 \mu\text{s}$ at the half-power points, the output pulse duration when lasing will depend on the level above threshold. Therefore, output energies, which are well defined and easily measured by intergrating, are plotted in Fig. 10 instead of output powers as is usually done. The spontaneous emission from 10-1-75 was significantly enhanced by emission from the Si-doped GaAs substrate. This was verified by visual examination of the near-field pattern with an infrared microscope and by a spectral scan of the output.

The equivalent thresholds in kA/cm^2 determined from the data in Fig. 10, i.e., where the straight line through the high pump energy data intersects the x -axis, are presented in Table II. From the fraction of the pump pulse absorbed by the active GaAs layers, ≈ 0.4 , the over-all external photon efficiency, the ratio of photons out of both ends of the sample to pump photons absorbed, and the external differential quantum efficiency, η_e , can be determined. Table II also give the external differential quantum efficiencies. There is some spread in the results shown in Table II. However, the qualitative differences between the various samples are substantiated by additional data obtained on other similar samples.

Absolute conversion efficiencies were also obtained at 8 K with multilayer samples 4-10-74-L ($l = 0.1734 \text{ cm}$) and 4-10-74-SS ($l = 0.0388 \text{ cm}$) using an optical pump at 7235 \AA . The two samples were identical except for their lengths. For these measurements, a single fixed cylindrical lens ($f = 30 \text{ cm}$) was used which produced a ribbonlike beam that was much longer than either sample so that the pump intensity was very nearly uniform and identical for both samples. The data are shown in Fig. 11. The resultant thresholds and differential quantum efficiencies are included in Table II.

The data in Fig. 11 can be analyzed to estimate the effective linear loss α since the external differential-photon and internal-photon efficiencies, η_e and η_i , respectively, should be related by¹⁵

$$\eta_e = \eta_i \{1 + \alpha l [\ln(1/R)]^{-1}\}^{-1} \quad (3)$$

The mirror power reflectivity and sample length are denoted by R and l , respectively. The values of η_e in

Table II lead to $\alpha = -0.5 \text{ cm}^{-1}$ which is, of course, meaningless. For α to be positive, the differential photon efficiency (slope) of the shorter sample (4-10-74-SS) must be larger than that of the longer sample. However, if the assumption is made that the differential photon efficiencies (slopes) can be in error by as much as 15%, it is estimated that $\alpha \approx 1 \text{ cm}^{-1}$. Similar results at low temperatures indicating very low losses have been obtained with other combinations of multilayer samples and under different focusing conditions. A low value of α might be expected for this sample since the active waveguide (see Table I) is 80% $\text{Al}_{0.2}\text{Ga}_{0.8}\text{As}$ which should be highly transparent at the lasing wavelength. The "internal photon efficiency", photons radiated per pump photon absorbed, estimated from the above value of α is approximately 15%. Since only part of the approximately triangular pump pulses is useful for laser action, the actual efficiencies are crudely estimated to be higher than quoted above by a factor of about 2.5, i.e., 35%.

The data in Fig. 11 can also be analyzed to give an indication of the dependence of the gain on the optical pump intensity via the expression¹⁶

$$\beta(j_{th})^b = \alpha + [\ln(1/R)]l^{-1}, \quad (4)$$

where β and b are constants to be determined, and j_{th} is the equivalent threshold current density. With $\alpha = 1$

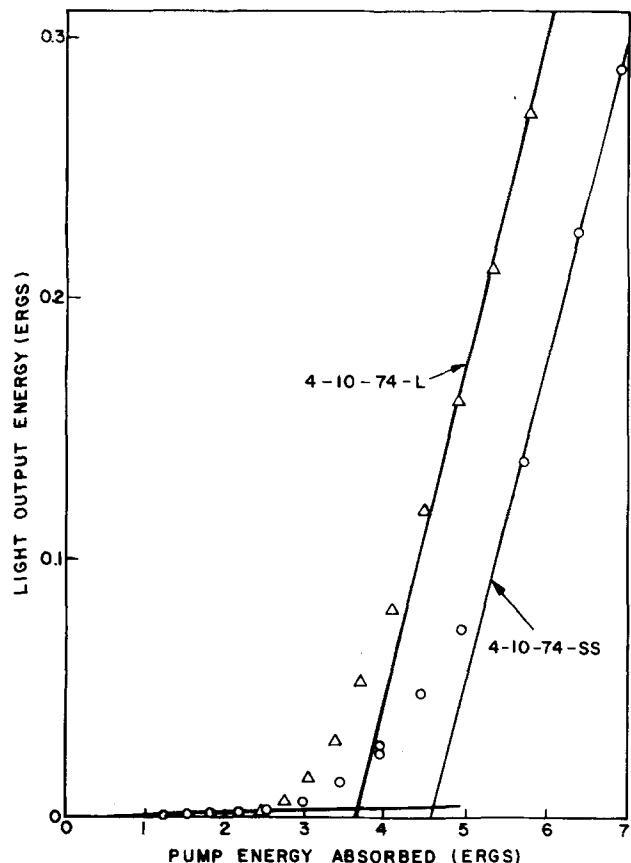


FIG. 11. Generated output optical energy versus absorbed pump optical energy at 7235 \AA at 8 K for two multilayer samples with 92-\AA -wide GaAs wells. Samples 4-10-74-SS and 4-10-74-L were 0.0388 and 0.1734 cm long, respectively.

cm^{-1} , $b = 0.8$. The thresholds calculated from the data in Fig. 11 can be combined with those in Fig. 3 to obtain additional estimates of b using the value $\alpha = 1 \text{ cm}^{-1}$. The average value of b , which is not very sensitive to α , is 0.8, in reasonable agreement with the value $b = 1$ reported earlier for injection lasers at low temperatures.^{17,18} The values of α and b determined from data obtained with this type of optical pumping should be viewed with caution due to the nonuniform temporal and spatial characteristics of the optical pump.^{6,7}

DISCUSSION

As has been discussed in some detail previously,^{6,7} the interpretation of some of the data obtained by this type of optical pumping technique is complicated by the Gaussian spatial dependence and approximately triangular temporal dependence of the optical pump pulses. Furthermore, random fluctuations in the pump intensity, perhaps $\pm 15\%$ from pulse to pulse under ideal conditions reduce the over-all quality of the data. The ideal pump should have the same uniform intensity for each pulse and be rectangular in the time domain as can be the case with injection pumping. With the present optical pumping technique, only the peak part of the pulse in the temporal and spatial domains is useful at or slightly above threshold. This explains the relatively high thresholds and low quantum efficiencies given in Table II compared to the equivalent quantities obtained with injection pumping of state-of-the-art DH GaAs- $\text{Al}_x\text{Ga}_{1-x}\text{As}$ lasers. For injection pumped DH's similar to the LPE units investigated here, $j_{\text{th}} \approx 2.5 \text{ kA/cm}^2$ and $\eta_e \approx 45\%$.¹⁹ The present values of j_{th} and η_e for the LPE DH samples are in reasonable agreement with those obtained by Rossi *et al.*⁷ who used a similar optical pumping technique for various units including DH. However, the most significant aspects of the data in Table II have to do with relative comparisons between the various structures investigated.

Another undesirable consequence of the present pumping technique is that a considerable fraction of the pump pulse goes into heating the sample. The resultant temperature increase at the lowest temperatures in the absence of thermal conduction is estimated to be of the order of 20 K for 1 erg of absorbed energy in a volume of the order of 10^{-8} cm^3 , which is typical of the samples studied. Although the process is surely not adiabatic as assumed above, these thermal effects might indeed make it difficult to observe the longitudinal modes. To change the longitudinal mode order $m = 2nl/\lambda$ by one-half requires a change of n of only 2×10^{-4} for a sample 0.1 cm long. The value of dn/dT is not known at these low temperatures. However, at room temperature $dn/dT \approx 3 \times 10^{-4}$ at the lasing wavelength for DH lasers,¹⁰ so that these considerations suggest that even small temperature changes while above threshold may have a detrimental effect on the visibility of longitudinal modes.

A number of comparisons between optically pumped LPE and MBE DH twins show that the room temperature MBE thresholds are about twice those obtained with similar LPE units, while the differential quantum effi-

ciencies are about one-half those observed with LPE-grown structures. Similar differences are also noted when comparing LPE and MBE units using injection pumping.⁸ However, the ML samples are inferior to all the DH units investigated, most notably when the GaAs wells are made thin, e.g., $\approx 100 \text{ \AA}$. Correcting the threshold data given in Table II for differences in the widths and the confinement factors²⁰ (≥ 0.91 in all cases) for the active waveguides does not significantly alter these general conclusions.

Crude estimates of optical gain using constant matrix elements, parabolic bands, and other assumptions that are known to be incorrect in detail for GaAs lasers, have suggested an enhanced gain for the ML structures when the GaAs wells are sufficiently thin, e.g., 100 \AA .²¹ The failure to observe this enhancement, if it indeed is realizable, may be due to the many additional GaAs- $\text{Al}_x\text{Ga}_{1-x}\text{As}$ interfaces in the ML samples and/or the generally recognized deficiencies of the laser-related characteristics of MBE-grown $\text{Al}_x\text{Ga}_{1-x}\text{As}$ layers.⁸ The improvement in the performance of the ML units investigated in this study over that reported previously¹ is ascribed to annealing of the 4-10-74 units and the new MBE system, mentioned earlier, that was used to grow the other samples. It appears that further improvements in the performance of the ML may have to await parallel advances in the growth of MBE material.

CONCLUSIONS

Extensive new data on optically pumped multilayer lasers grown by MBE demonstrate that the inherent quantum effects are indeed still present under lasing conditions at room temperature. However, the lasing thresholds and quantum efficiencies of the multilayer units are inferior to those of conventional MBE double-heterostructure lasers. In addition, LPE double-heterostructure lasers are about a factor of 2 better with regard to thresholds and differential quantum efficiencies than their MBE twins.

ACKNOWLEDGMENTS

The authors would like to thank Dr. H.C. Casey, Jr. and Dr. F.K. Reinhart for numerous informative discussions on various aspects of this work.

- ¹J. P. van der Ziel, R. Dingle, R. C. Miller, W. Wiegmann, and W. A. Nordland, Jr., *Appl. Phys. Lett.* **26**, 463 (1975).
- ²R. Dingle, W. Wiegmann, and C. H. Henry, *Phys. Rev. Lett.* **33**, 827 (1974).
- ³R. Tsu and L. Esaki, *Appl. Phys. Lett.* **22**, 562 (1973).
- ⁴R. Dingle, A. C. Gossard, and W. Wiegmann, *Phys. Rev. Lett.* **34**, 1327 (1975).
- ⁵A. Y. Cho, *J. Vac. Sci. Technol.* **8**, S31 (1971).
- ⁶S. R. Chinn, J. A. Rossi, C. M. Wolfe, and A. Mooradian, *IEEE J. Quantum Electron.* **QE-9**, 294 (1973).
- ⁷J. A. Rossi, S. R. Chinn, J. J. Hsieh, and M. C. Fim, *J. Appl. Phys.* **45**, 5383 (1974).
- ⁸A. Y. Cho, R. W. Dixon, H. C. Casey, Jr., and R. L. Hartman, *Appl. Phys. Lett.* **28**, 501 (1976).

- ⁹R. Dingle, in *Festkörperprobleme (Advances in Solid State Physics)*, edited by H.J. Quiesser (Pergamon/Vieweg, Braunschweig, 1975), Vol. XV, p. 21.
- ¹⁰F. K. Reinhart (private communication).
- ¹¹F. K. Reinhart, I. Hayashi, and M. B. Panish, *J. Appl. Phys.* **42**, 4466 (1971).
- ¹²C. D. Thurmond, *J. Electrochem. Soc.* **122**, 1133 (1975).
- ¹³J. Camassel, D. Auvergne, and H. Mathieu, *J. Appl. Phys.* **46**, 2683 (1975).
- ¹⁴M. I. Nathan, A. B. Fowler, and G. Burns, *Phys. Rev. Lett.* **11**, 152 (1963).
- ¹⁵J. Shah, R. F. Leheny, and C. Lin, *Solid State Commun.* **18**, 1035 (1976).
- ¹⁶I. R. Biard, W. N. Carr, and B. S. Reed, *Trans. AIME* **230**, 286 (1964).
- ¹⁷G. Lasher and F. Stern, *Phys. Rev.* **133**, A553 (1964).
- ¹⁸F. Stern, in *Laser Handbook*, edited by F. T. Arecchi and E. O. Schulz-DuBois (North-Holland, Amsterdam, 1972), Vol. 1, Chap. B4.
- ¹⁹M. B. Panish, *IEEE Trans. Microwave Theory Tech.* **MTT-23**, 20 (1975).
- ²⁰F. Stern, *Phys. Rev.* **148**, 186 (1966).
- ²¹R. Dingle and C. H. Henry (private communication).